J. Inst. Eng. India Ser. E (June 2020) 101(1):53–60
https://doi.org/10.1007/s40034-019-00154-0

ORIGINAL CONTRIBUTION

Fish-Bone-Doped Sea Shell for Biodiesel Production from Waste Cooking Oil

S. Niju[1] · M. Kirthikaa[1] · S. Arrthi[1] · P. Dharani[1] · S. Ramya[1] · M. Balajii[1]

Received: 18 December 2017 / Accepted: 25 November 2019 / Published online: 30 November 2019

Abstract Transesterification of waste cooking oil with methanol using calcined waste fish bone and sea shell catalyst was studied. An inexpensive and environmentally benign catalyst was prepared from waste fish bones (WFB) and *Tellina tenuis* shells (TTS), and the catalyst was characterized by Fourier transform infrared spectroscopy (FTIR), scanning electron microscopy (SEM), Brunauer–Emmett–Teller, X-ray diffraction (XRD) and energy-dispersive X-ray spectroscopy (EDS) techniques. From XRD, it was confirmed that the major phase of WFB was hydroxyapatite and calcium oxide was found to be the dominant fraction of calcined TTS. FTIR and SEM–EDS analysis of WFB confirmed the presence of hydroxyapatite exhibiting hexagonal structure. Different combinations of WFB and TTS have been developed to obtain novel catalyst composition. Above 94% conversion was reported with various combinations of WFB and TTS using 3 wt% catalyst, 12:1 molar ratio, 65 °C and 1.5 h.

Keywords Fish bone · Heterogeneous catalyst · Triglycerides · Waste cooking oil · Biodiesel

Introduction

The energy demand of the world is hugely met by the fossil fuel reserves, and these reserves are declining day to day due to rapid consumption. The scarcity of crude oil leads to an increase in the price of crude oil in the world market [1]. Also, rapid use of these resources would also have a negative impact on the environment by the emission of greenhouse gases such as carbon dioxide, sulfur dioxide, carbon monoxide, nitrogen oxide and other particulate matters [2]. In order to reduce the effect of these impacts on the environment, researchers have started to focus on alternative sources of energy. Biofuels are one such alternative source which is derived from biological sources. Among the various biofuels, biodiesel can be used as a replacement for conventional diesel that is derived from fossil fuels. Different methods of biodiesel production are direct use (blending), pyrolysis, microemulsion and transesterification [3]. The most common method of biodiesel production is transesterification in which triglycerides present react with methanol in the existence of catalyst to produce esters and glycerol [4].

Both edible and non-edible lipidic feedstocks have been employed for biodiesel synthesis. It has been estimated that 75% of the entirety production cost is contributed by the feedstock. Edible oils (soybean oil, sunflower oil, rapeseed oil, sesame oil, etc.) which are available from the agricultural sector are the most widely used feedstocks for biodiesel production. Edible oil alone contributes to 95% of the global biodiesel synthesis [5]. However, the continuous usage of comestible crops for the production of biodiesel is limited due to food versus fuel disputes. Hence, non-comestible oils (second generation) can be employed as an alternative to edible oil since the edible oil has huge demand as fodder and also it was expensive [6]. The second-generation oil feedstocks include neem (*Azadirachta indica*), tobacco seed (*Nicotiana tabacum* L.), mahua (*Madhuca indica*), karanja (*Pongamia pinnata*), jatropha tree (*Jatropha curcas*), polanga (*Calophyllum inophyllum*) and castor (*Ricinus communis*) [7–10]. Employing non-edible oils for biodiesel production requires additional land

✉ S. Niju
sn.bio@psgtech.ac.in; nijuwillbe@gmail.com

[1] Department of Biotechnology, PSG College of Technology, Coimbatore, Tamilnadu 641004, India

(farm fields) to grow, and also, it involves a two-step esterification and transesterification process which predominantly increases the production cost. However, utilizing WCO as a lipid feedstock will reduce the production cost, thereby making the process more efficient and economical. In addition, it significantly diminishes the environmental pollution aroused due to the disposal. In recent years, the usage of WCO as a feedstock in biodiesel synthesis has been highlighted by several scientists worldwide [11–15].

Catalysts can be grouped into heterogeneous and homogeneous catalysts. The homogeneous catalysts are broadly exercised in large-scale production due to faster reaction rate, higher yield and mild reaction condition, and the broadly used homogeneous catalysts are potassium hydroxide, sodium hydroxide, sodium methoxide and potassium methoxide [16]. Though there are many advantages, the major restriction is that the process is not environmentally benign and cost-effective. The amount of wastewater generated during the purification of biodiesel is enormous which may have serious effects on the environment. During homogeneous catalyst-based transesterification, the separation of glycerol from the end product (biodiesel) requires a lengthy process and distillation for purification [17]. To overcome the drawbacks of a homogeneous catalyst, the heterogeneous catalyst is being explored widely. Heterogeneous catalysts are subsumed under green technology because of their recyclability, efficient downstream processing steps and lesser water requirement for product purification. Some of the heterogeneous catalysts that are used for laboratory-scale biodiesel production include enzyme-based catalyst, leftover-based heterogeneous catalysts, transition metal oxides and derivatives, alkaline earth metal oxides and derivatives, alkali metal oxides and derivatives, mixed metal oxides and derivatives, boron group-based heterogeneous catalyst, ion exchange resin-type acid heterogeneous catalyst, carbon-based heterogeneous catalysts and sulfated oxide acid heterogeneous catalyst [18].

Among various groups of heterogeneous catalysts, CaO-based catalyst is gaining a huge attention owing to its advantages such as huge availability, very less solubility in alcohols and environmentally friendly and non-toxic nature. Recently, several research works have been experimented by utilizing various CaO sources such as conch shell [19], river snail shell [20], ostrich egg shell and chicken egg shell [21],white bivalve clam shell [22], *Gallus domesticus* shells [23], mussel shell [24], *Tellina tenuis* [25], waste scallop shell [26] and crab shell [27]. In the present study, to make the process more cost-effective and environmentally friendly waste materials such as WFB and TTS were mixed in different proportions to obtain novel catalyst composition and tested to find the catalytic activity in transesterification reaction.

Materials and Methods

Materials

WFB were collected from a local restaurant in Coimbatore, and TTS were collected from the seashore of Tuticorin. WCO was acquired from hostel canteen, PSG College of Technology, Coimbatore, Tamil Nadu, India, and it was filtered to eliminate the solid debris. Then, it was heated to evaporate the possible water content and kept in an airtight bottle. The physiochemical analysis on WCO was performed and is illustrated in Table 1. Standard titration method was employed to determine the acid value of oil [28] and the value was found to be low. Hence, WCO can be used directly for the transesterification process. Analytical grade reagents and chemicals were utilized and purchased from S.D. Fine Chemicals Ltd., Mumbai.

Preparation of Catalyst

WFB and TTS were initially rinsed with normal water to remove the unsolicited substance remaining on the surface and then cleansed with deionized water. Then, the washed materials were dehydrated in an oven overnight at 105 °C. Dried WFB and TTS were crushed into fine particles and calcined in a box furnace under limited oxygen at 900 °C for 3 h [19, 25] separately to remove organic impurities, and the calcined catalysts were indicated as WFB-900 and TTS-900. In order to obtain different combinations of WFB and TTS in a highly active form (100% WFB, 90% WFB-10% TTS, 80% WFB-20% TTS, 70% WFB-30% TTS, 60% WFB-40% TTS, 50% WFB-50% TTS, 40% WFB-60% TTS, 30% WFB-70% TTS, 20% WFB-80% TTS, 10% WFB-90% TTS and 100% TTS), WFB-900 and TTS-900 were refluxed with deionized water for 2 h in a constant-temperature water bath at 60 °C. The slurry was filtered and the solid particles were dehydrated at 600 °C by calcination process [29, 30]. The newly obtained catalysts were labeled and are presented in Table 2.

Catalyst Characterization

The catalyst was characterized using XRD, FTIR, BET, SEM and EDS techniques. XRD patterns of the catalyst were determined using an X-ray diffractometer (PANalytical X'Pert 3 Powder, Netherlands) using Cu as an anode material at 30 mA and 45 kV. Samples were scanned in the 2θ range varying from 10.00 to 89.99. The surface morphology was investigated by using FESEM with EDS (Carl

Table 1 Physicochemical properties of WCO used in the present study

Properties	Measured values
Density at 25 °C (kg/m^3)	923
Kinematic viscosity at 40 °C (mm^2 s^{-1})	28.55
Acid value (mg of KOH/gm of oil)	1.12

Table 2 Different combinations of WFB and TTS

TTS (w/w)%	WFB (w/w)%	Name of the catalyst obtained
0	100	WFB_{100}-900-600
10	90	WFB_{90}–TTS_{10}-900-600
20	80	WFB_{80}–TTS_{20}-900-600
30	70	WFB_{70}–TTS_{30}-900-600
40	60	WFB_{60}–TTS_{40}-900-600
50	50	WFB_{50}–TTS_{50}-900-600
60	40	WFB_{40}–TTS_{60}-900-600
70	30	WFB_{30}–TTS_{70}-900-600
80	20	WFB_{20}–TTS_{80}-900-600
90	10	WFB_{10}–TTS_{90}-900-600
100	0	TTS_{100}-900-600

Zeiss Microscopy Ltd, Sigma, UK), with an accelerating voltage of 0.2–30 kV. Surface area was measured by using the N2 adsorption–desorption technique (NOVA 2200, Quantachrome, USA). The porosity and surface area were analyzed at the boiling point of the nitrogen—195.6 °C. Before nitrogen desorption, the sample was degassed at 200 °C for 12 h under vacuum conditions. FTIR spectrum was recorded using a FTIR spectrophotometer (Thermo Scientific Ltd., USA). FTIR spectrum was recorded in the range 4000–600 cm^{-1}.

Transesterification Reaction

The transesterification reaction was performed in a 500-ml three-necked reactor. One of the necks was fitted with a temperature indicator, the central neck was fitted with a motor-driven agitator, and other neck was attached to a water-circulated condenser. The catalyst was introduced into the reactor followed by the addition of methanol and WCO. Based on preliminary studies carried out using one-variable-at-a-time method, all the reactions were performed at 12:1 ratio of methanol to oil, 3wt% catalyst, for 1.5 h. The transesterification temperature and the stirrer speed were kept at 65 °C and 450 rpm, respectively, based on the previously reported studies [19, 31]. After transesterification reaction was completed, the catalyst was separated from the fatty acid methyl ester (FAME) and glycerol by overnight filtration process using No. 1 Whatman filter paper. The top most layer was labeled as FAME, and the bottom deposit was characterized as glycerol. % FAME conversion was estimated by proton nuclear magnetic resonance spectroscopy (^{1}H-NMR, 300 MHz Bruker Avance II, Switzerland) using the Knothe equation [32]. ^{1}H-NMR was exercised to determine methyl ester conversion via the signal amplitude proportionate to the hydrogen nuclei numbers comprised in biodiesel. The methylene protons emerge at 2.3 ppm, while the protons of methoxy groups exist at 3.7 ppm, and these two signals confirmed the occurrence of methyl esters. Maximum peaks arise between 0 and 5 ppm in spectra, while the unsaturated arrangements exist between 5 and 9 ppm.

$$\%\text{FAME conversion} = \left(\frac{2A_{\text{ME}}}{3A_{\alpha-\text{CH}_2}}\right) \times 100 \quad (1)$$

$A_{\alpha\text{-CH2}}$ is the integration value of α-methylene protons, A_{ME} integration value of methoxy protons and % FAME conversion % triglycerides conversion into methyl ester.

The factor 2 represents the number of protons on methylene, while the factor 3 corresponds to the number of protons on methyl ester. Furthermore, the synthesized FAME was characterized using gas chromatography (GC, make: Systronics, India; model: GC2010) with a 30-m-long fused silica capillary column (Omegawax$^{\text{TM}}$ 320). Nitrogen was employed as carrier gas. Injector was initially maintained at 100 °C for 2 min and it was ramped to 260 °C at 1.5 °C per min, while the detector (flame ionization detector, FID) temperature was set at 260 °C. A 100-mg FAME mix (C8-C24 standard, CRM18918 SUPELCO) purchased from Sigma-Aldrich was used for identification of methyl esters existing in the synthesized FAME.

Results and Discussion

Characterization of Calcined Fish Bone

SEM analysis of the fish bone calcined at 900 °C for 3 h was performed, and the morphology was studied at different magnifications (5000×, 20,000× and 50,000×) and is presented in Fig. 1a–c, respectively. At lower magnifications, the sample appears as a cluster of hexagonal nanorods, and as the magnification increases, the hexagonal shape of the sample can be visualized clearly and confirmed as hydroxyapatite. Khalil et al. [33] also reported the SEM image of hydroxyapatite as a hexagonal shape in structure. Elemental analysis was performed by EDS and is presented in Fig. 2. It can be seen that calcium forms the highest peak at 3.7 keV. The weight percentage of calcium

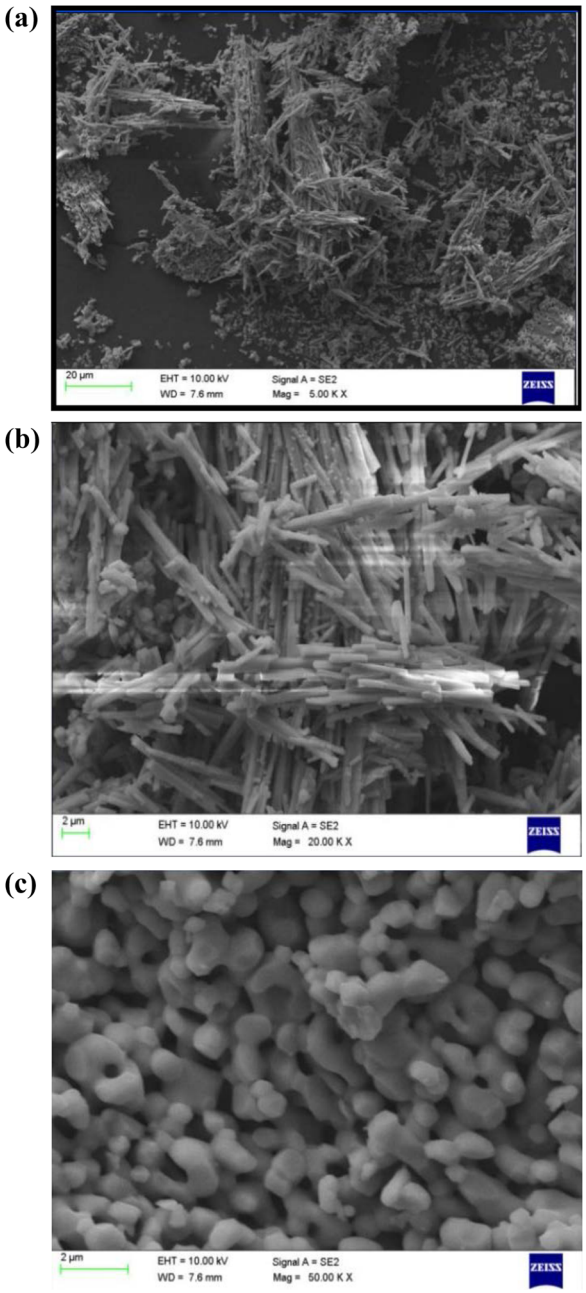

Fig. 1 **a** SEM image of the calcined fish bone with 5000× magnification. **b** SEM image of the calcined fish bone with 20,000× magnification. **c** SEM image of the calcined fish bone with 50,000× magnification

oxide is the highest being 60.46%, which indicates that it is the major compound in the sample followed by phosphorus pentoxide with 37.92%. To find the crystallinity of calcined fish bone, XRD analysis was performed and is presented in Fig. 3. The diffraction peaks were identified using a standard JCPDS file. The highest peaks were obtained at angles $2\theta = 31.75°$ and $2\theta = 33.85°$. By comparing the obtained peaks with JCPDS data, the peaks obtained were confirmed as hydroxyapatite. Moreover, the peaks obtained at 2θ

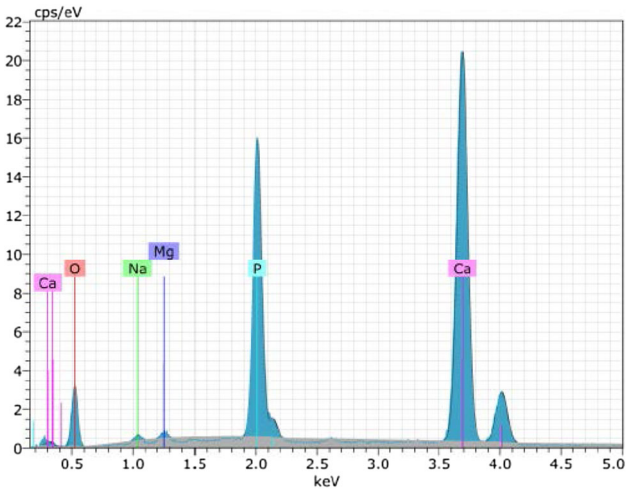

Fig. 2 EDS analysis of the calcined fish bone

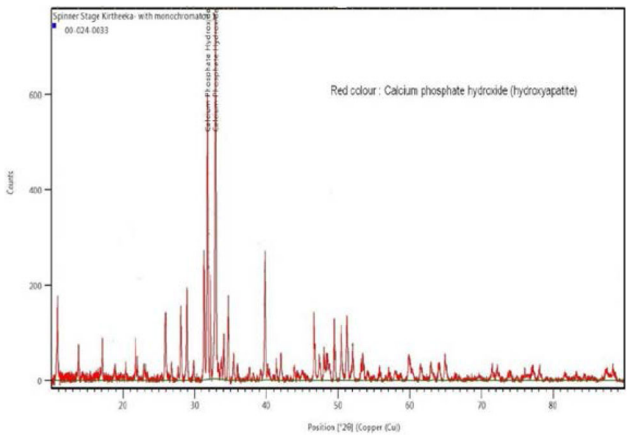

Fig. 3 XRD pattern of the calcined fish bone

values of 10.84, 21.77, 25.90, 32.85, 39.77, 46.64 and 62.90 were compared with the literature [12, 13] and the observations confirmed the presence of hydroxyapatite. FTIR analysis was used to characterize the different functional groups of hydroxyapatite. The spectrum was recorded in the range of 4000–600 cm^{-1} and is presented in Fig. 4. The formation of hydroxyapatite is indicated by the broad range complex band at 1000–1100 cm^{-1} due to asymmetric stretching form of vibration for phosphate groups as confirmed by Cahyanto et al [34] and Mondal et al. [35]. A band detected at 961.19 cm^{-1} indicates the existence of phosphate ions as confirmed by Rehman et al. [36]. A sharp band observed at 1086.15 cm^{-1} indicates the stretching mode of PO_4^{3-} as confirmed by Arsad et al. [37]. A slight formation of the peak at 3571 cm^{-1} indicates the mild presence of OH functional groups. The absence of peaks at 875 cm^{-1}, 1416 cm^{-1} and 1461 cm^{-1} indicates complete calcination because of the absence of carbonate ions. BET analysis was performed to study the surface

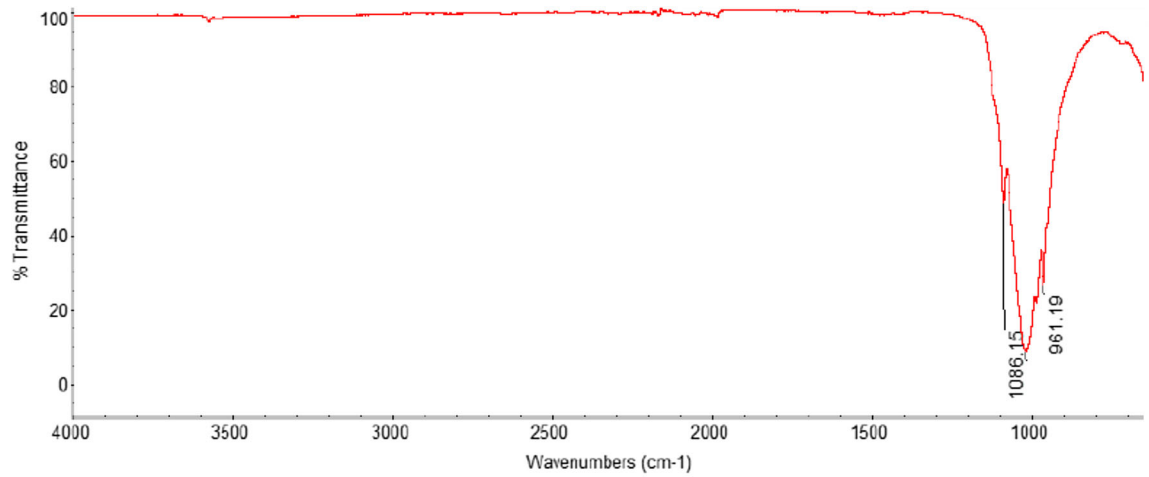

Fig. 4 FTIR pattern of the calcined fish bone

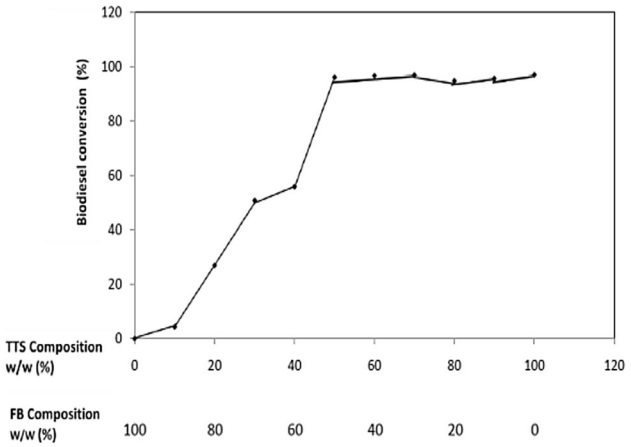

Fig. 5 Variation of biodiesel conversion with different combinations of WFB and TTS

area, and the surface area of calcined fish bone was determined as 1.42 m^2/g. Characterization results of TTS were reported by Niju et al. [25] in their previous studies.

Catalyst Activity Comparison for Various Combinations of WFB–TTS Catalysts

Transesterification experiments were carried out in a 500-ml three-necked flask stationed in an invariable temperature bath using WFB_{100}-900-600, WFB_{90}–TTS_{10}-900-600, WFB_{80}–TTS_{20}-900-600, WFB_{70}–TTS_{30}-900-600, WFB_{60}–TTS_{40}-900-600, WFB_{50}–TTS_{50}-900-600, WFB_{40}–TTS_{60}-900-600, WFB_{30}–TTS_{70}-900-600, WFB_{20}–TTS_{80}-900-600, WFB_{10}–TTS_{90}-900-600 and TTS_{100}-900-600. All the reactions were performed with 3 wt% catalyst, 12:1 ratio at 65 °C for 1.5 h. The catalyst was removed from the FAME–glycerol mixture by filtration after completion, and biodiesel was stored for further analysis to find the formation of methyl esters. The conversion of WCO into biodiesel was quantified using ^{1}H-NMR based on the integration signals of methoxy proton of the methyl ester at 3.7 ppm and α-methylene proton of the fatty acid derivative at 2.3 ppm. From the ^{1}H-NMR results, it has been observed that biodiesel conversion increased with different combinations of WFB–TTS as indicated in Fig. 5. The ^{1}H-NMR and GC spectrum of the biodiesel catalyzed by WFB_{50}–TTS_{50}-900-600 is presented in Figs. 6 and 7, respectively. WFB_{50}–TTS_{50}-900-600 catalyst (50 w/w% WFB-50 w/w% TTS) gives a biodiesel conversion of 95.87% and the other combinations consistently obtained a biodiesel conversion of above 94%. Hence, in the present work, WFB_{50}–TTS_{50}-900-600 catalyst combination was observed as appropriate composition for biodiesel synthesis. Moreover, the biodiesel conversion obtained using WFB–TTS catalyst was compared with the state of the art in the literature and is given in the following table. From Table 3, it is clear that the reported results required a higher ratio of methanol to oil, high catalyst loadings and prolonged reaction time compared to the present work. Therefore, a mixture of WFB and TSS provides a new technique to enhance the catalytic activity of transesterification reaction in biodiesel production. The fatty acid composition of the synthesized biodiesel is presented in Table 4.

Conclusion

The present work revealed that impregnation of TTS with WFB using hydration–dehydration technique is a new and effective method to enhance the catalytic activity of waste materials in the transesterification process for biodiesel production. Waste materials such as seashells and fish bones are rarely used for the development of practical products, and hence, the utilization of these waste materials

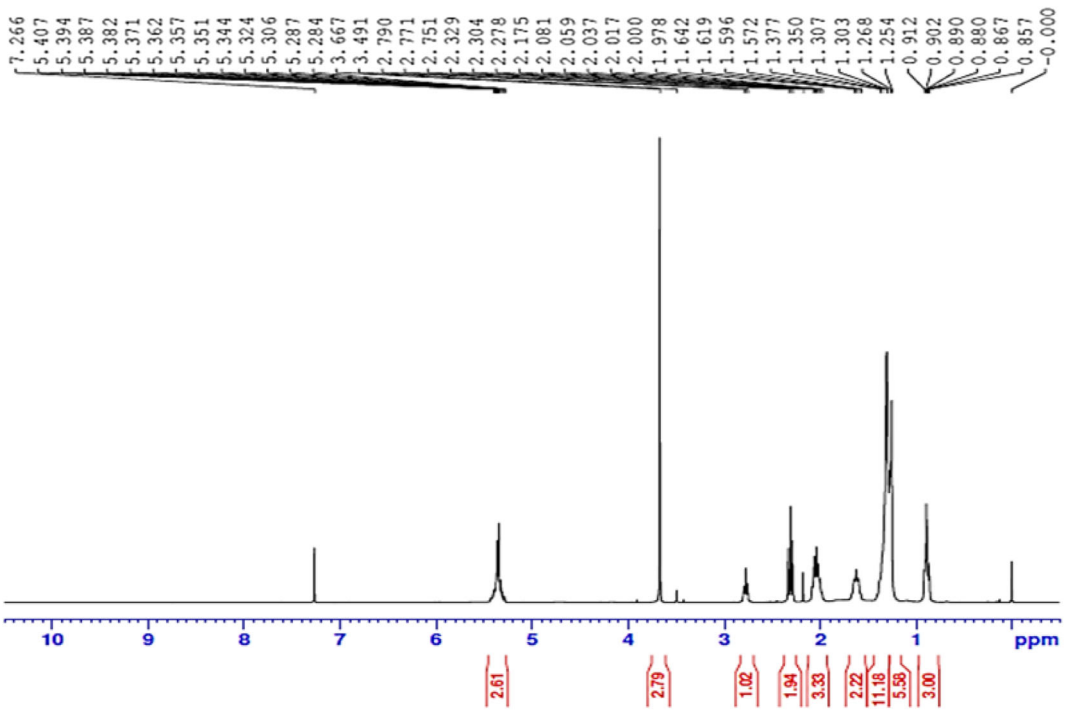

Fig. 6 ^{1}H-NMR spectrum of the biodiesel catalyzed by WFB_{50}–TTS_{50}-900-600

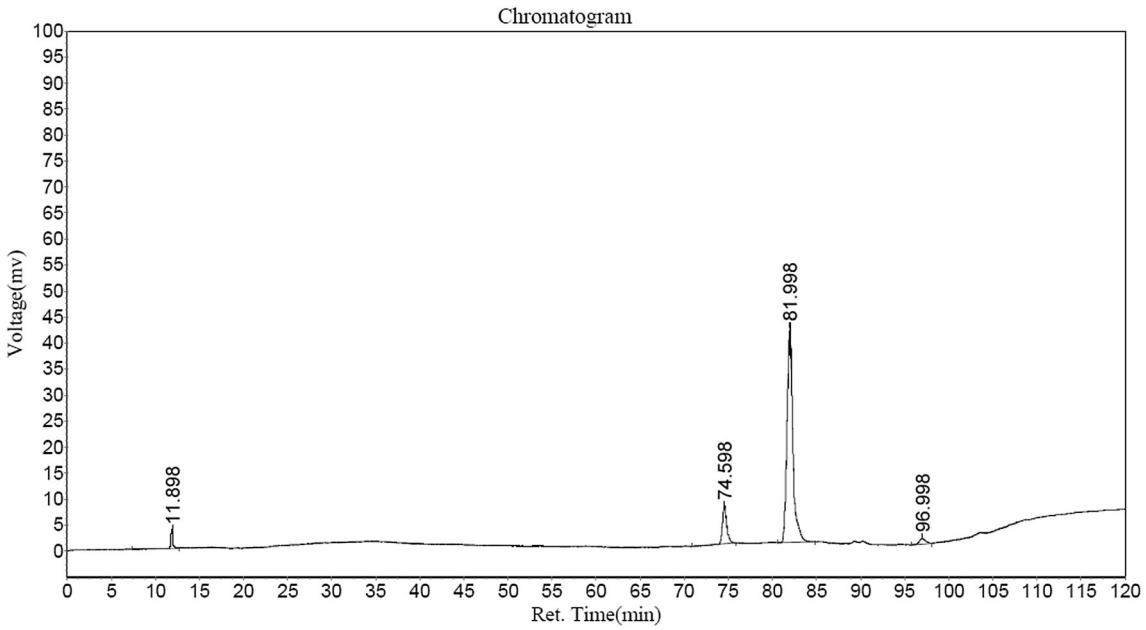

Fig. 7 GC spectrum of the biodiesel catalyzed by WFB_{50}–TTS_{50}-900-600

as a solid catalyst will help sustainable development. Biodiesel synthesis using WCO as a feedstock and waste materials as a solid catalyst will eliminate the waste disposal problem and diminish the biodiesel cost, rendering biodiesel a feasible substitute fuel to conventional diesel. Different combinations of WFB and TTS were tested for WCO transesterification, and a high conversion of about 95.87% was obtained using 50(w/w)% WFB and 50 (w/w)% TTS with 3 wt% catalyst, 12:1 methanol-to-oil ratio at 65 °C for 1.5 h.

Table 3 Performance evaluation of WFB–TTS catalyst with the state of the art in the literature

Catalyst used	Feedstock used	Optimum transesterification reaction conditions				Yield/conversion (%)
		Methanol/oil molar ratio	Amount of catalysts (wt%)	Temperature (°C)	Time (h)	
Waste animal bone [38]	Palm oil	18:1	20	65	4	96.78
Pork bone [39]	Jatropha oil	18:1	4	150–800 W (microwave power)	0.083	93.88
$AlNO_3$-doped cooked waste fish bones [40]	Neem oil	1:30	1	90	4	97.26
Fish scale-supported Ni catalyst [41]	Waste frying soybean oil	20:1	30	65	4	98.4
Chicoreus brunneus shells [42]	Rice bran oil	30:1	0.4	65	2	93
Gallus domesticus shells [23]	Waste palm oil	15:1	3	80	3	90.1
Turbo jourdani shells [43]	Palm oil	3:1	10	80 ± 5	7	> 99
Sulfated tin oxide [44]	*Moringa oleifera* oil	1:19.5	3	150	2.5	84
Conch shells [19]	*Moringa oleifera* oil	8.66:1	8.02	65	2.17	97.06
Pomacea shells [45]	Palm oil	7:1	4	60	4	95.61
Anadara granosa[1] and *Paphia undulata*[2] shells [46]	Palm oil	12:1	6	60	2	92[1] and 94[2]
Angel wing shells [47]	Microalgae *Nannochloropsis oculata* oil	150:1 wt ratio	9	65	1	84.11
CaO nanoparticles [48]	*Ceiba pentandra* oil	10.37:1	1.5	65	70.52 min	96.2
Boiler scale deposits [49]	Jatropha oil	12:1	8	65	3	82.85
Ostrich eggshell* and chicken eggshell[#] [21]	Used cooking oil	12:1	1.5	65	2	96* and 94[#]
Waste obtuse horn shell [50]	Palm oil	12:1	5	–	6	86.75
White bivalve clam shell [29]	Waste frying oil	12:1	7	65	1	94.25
Flamboyant pods [51]	*Hevea brasiliensis* oil	15:1	3.5	55	1	89.81
Mesua ferrea Linn seeds [52]	*Mesua ferrea* oil	6:1	10	55	2	95.57
Eggshell ash [12]	Waste vegetable oil	22.5:1	3.5	65 ± 5	5.5	91
Chicken manure [15]	Waste cooking oil	15:1	7.5	65	6	90.8
Fluorite [53]	Rubber seed oil	12:1	4	65	5	95.95%
WFB–TTS (present work)	Waste cooking oil	12:1	3	65	1.5	95.7

1, 2, *, & # represents the biodiesel yield or conversion when the respective catalyst employed during the reaction

Table 4 Fatty acids identified in the synthesized biodiesel

Compound name	Retention time (min)	Percentage (%)
Methyl octanoate	11.898	2.59
Methyl palmitate	74.598	11.22
Cis-9-Oleic acid methyl ester	81.998	83.74
Methyl lignocerate	96.998	2.44

References

1. A.K. Agarwal, Prog. Energy Combust. Sci. **33**, 233 (2007)
2. G. Baskar, R. Aiswarya, Renew. Sustain. Energy Rev. **57**, 496 (2016)
3. A. Demirbas, Energy Convers. Manag. **49**, 125 (2008)
4. J.M. Marchetti, V.U. Miguel, A.F. Errazu, Renew. Sustain. Energy Rev. **11**, 1300 (2007)
5. M.M. Gui, K.T. Lee, S. Bhatia, Energy **33**, 1646 (2008)
6. A.A. Refaat, Int. J. Environ. Sci. Technol. **7**, 183 (2010)
7. M. Balat, Energy Convers. Manag. **52**, 1479 (2011)
8. K. Ramezani, S. Rowshanzamir, M.H. Eikani, Energy **35**, 4142 (2010)
9. B. Karmakar, S.H. Dhawane, G. Halder, J. Environ. Chem. Eng. **6**, 2684 (2018)
10. F.A. Dawodu, O. Ayodele, J. Xin, S. Zhang, D. Yan, Appl. Energy **114**, 819 (2014)
11. S.H. Dhawane, B. Karmakar, S. Ghosh, G. Halder, J. Environ. Chem. Eng. **6**, 3971 (2018)
12. N. Tshizanga, E.F. Aransiola, O. Oyekola, S. Afr. J. Chem. Eng. **23**, 145 (2017)
13. M. Farooq, A. Ramli, A. Naeem, Renew. Energy **76**, 362 (2015)
14. M. Babaki, M. Yousefi, Z. Habibi, M. Mohammadi, Renew. Energy **105**, 465 (2017)

15. T. Maneerung, S. Kawi, Y. Dai, C.H. Wang, Energy Convers. Manag. **123**, 487 (2016)
16. L. Bournay, D. Casanave, B. Delfort, G. Hillion, J.A. Chodorge, Catal. Today **106**, 190 (2005)
17. M. Canakci, J. Van Gerpen, Am. Soc. Agric. Eng. **44**, 1429 (2001)
18. A.P.S. Chouhan, A.K. Sarma, Renew. Sustain. Energy Rev. **15**, 4378 (2011)
19. S. Niju, C. Anushya, M. Balajii, Environ. Prog. Sustain. Energy **1**, 12 (2018)
20. S. Kaewdaeng, P. Sintuya, R. Nirunsin, Energy Procedia **138**, 937 (2017)
21. Y.H. Tan, M.O. Abdullah, C. Nolasco-Hipolito, Y.H. Taufiq-Yap, Appl. Energy **160**, 58 (2015)
22. N. Girish, S.P. Niju, K.M. Meera Sheriffa Begum, N. Anantharaman, Fuel **111**, 653 (2013)
23. N. Mansir, S.H. Teo, U. Rashid, Y.H. Taufiq-Yap, Fuel **211**, 67 (2018)
24. H. Hadiyanto, A.H. Afianti, U.I. Navi'a, N.P. Adetya, W. Widayat, H. Sutanto, J. Environ. Chem. Eng. **5**, 4559 (2017)
25. S. Niju, J. Indhumathi, K.M.M.S. Begum, N. Anantharaman, Biofuels **8**, 1 (2016)
26. S. Sirisomboonchai, M. Abuduwayiti, G. Guan, C. Samart, S. Abliz, X. Hao, K. Kusakabe, A. Abudula, Energy Convers. Manag. **95**, 242–247 (2015)
27. V. Shankar, R. Jambulingam, Sustain. Environ. Res. **27**, 273 (2017)
28. S. Mahajan, S.K. Konar, D.G.B. Boocock, JAOCS, J. Am. Oil Chem. Soc. **83**, 567 (2006)
29. S. Niju, K.M. Meera Sheriffa Begum, N. Anantharaman, Arab. J. Chem. **9**, 633 (2016)
30. B. Yoosuk, P. Udomsap, B. Puttasawat, P. Krasae, Bioresour. Technol. **101**, 3784 (2010)
31. S. Niju, K.M.M. Sheriffa Begum, N. Anantharaman, Environ. Prog. Sustain. Energy **34**, 248 (2015)
32. G. Knothe, JAOCS, J. Am. Oil Chem. Soc. **83**, 823 (2006)
33. K.A. Khalil, A.A. Almajid, M.S. Soliman, Mater. Sci. Appl. **02**, 105 (2011)
34. Z. Cahyanto, A. Kosasih, E. Aripin, D. Hasratiningsih, IOP Conf. Ser. Mater. Sci. Eng. **172**, 012006 (2017)
35. S. Mondal, B. Mondal, A. Dey, S.S. Mukhopadhyay, J. Miner. Mater. Charact. Eng. **11**, 55 (2012)
36. I. Rehman, W. Bonfield, J. Mater. Sci. Mater. Med. **8**, 1 (1997)
37. P. M. L. Maisara, S.M. Arsad, in *2nd International Conference on Biotechnology and Food Science*, vol. 7 (2011), p. 184
38. A. Obadiah, G.A. Swaroopa, S.V. Kumar, K.R. Jeganathan, A. Ramasubbu, Bioresour. Technol. **116**, 512 (2012)
39. A. Buasri, T. Inkaew, L. Kodephun, W. Yenying, V. Loryueny-ong, Key Eng. Mater. **659**, 216 (2015)
40. H. Sahu, K. Mohanty, Chem. Eng. J. **280**, 564 (2015)
41. R. Chakraborty, S. Bepari, A. Banerjee, Bioresour. Technol. **102**, 3610 (2011)
42. H. Mazaheri, H.C. Ong, H.H. Masjuki, Z. Amini, M.D. Harrison, C.T. Wang, F. Kusumo, A. Alwi, Energy **144**, 10 (2018)
43. S. Boonyuen, S.M. Smith, M. Malaithong, A. Prokaew, B. Cherdhirunkorn, A. Luengnaruemitchai, J. Clean. Prod. **177**, 925 (2018)
44. G. Kafuku, M.K. Lam, J. Kansedo, K.T. Lee, M. Mbarawa, Fuel Process. Technol. **91**, 1525 (2010)
45. Y.Y. Margaretha, H.S. Prastyo, A. Ayucitra, S. Ismadji, Int. J. Energy Environ. Eng. **3**, 33 (2012)
46. H.H. Sri, P. Lestari, A.A.W. Widayat, H. Sutanto, H. Hadiyanto, S.P. Lestari, A. Abdullah, W. Widayat, H. Sutanto, Int. J. Energy Environ. Eng. **7**, 297 (2016)
47. O. Nur Syazwani, U. Rashid, Y.H. Taufiq Yap, Energy Convers. Manag. **101**, 749 (2015)
48. H.R. Harsha Hebbar, M.C. Math, K.V. Yatish, Energy **143**, 25 (2018)
49. Y. Eswararao, S. Niju, K.M.M.S. Begum, N. Anantharaman, Biofuels **7**, 1 (2017)
50. S.L. Lee, Y.C. Wong, Y.P. Tan, S.Y. Yew, Energy Convers. Manag. **93**, 282 (2015)
51. S.H. Dhawane, T. Kumar, G. Halder, Renew. Energy **89**, 506 (2016)
52. A.P. Bora, S.H. Dhawane, K. Anupam, G. Halder, Renew. Energy **121**, 195 (2018)
53. B.A.V.S.L. Sai, S. Niju, B.K.M. Meera, N. Anantharaman, Energy Sources Part A Recover. Util. Environ. Eff. **41**, 1 (2018)